Brazilian Journal
of Chemical
Engineering

ISSN 0104-6632
Printed in Brazil
www.abeq.org.br/bjche

Vol. 26, No. 03, pp. 493 - 502, July - September, 2009

TOTAL CATALYTIC WET OXIDATION OF PHENOL AND ITS CHLORINATED DERIVATES WITH MnO_2/CeO_2 CATALYST IN A SLURRY REACTOR

A. J. Luna[1*], L. O. A. Rojas[2], D. M. A. Melo[3], M. Benachour[4] and J. F. de Sousa[2]

[1]Instituto Nacional de Propriedade Industrial, R. Mayrink Veiga 9, 19º andar, Centro,
CEP: 20090-910, Phone: + (55) (21) 2139-3767, Rio de Janeiro - RJ, Brazil.
E-mail: airtonj@inpi.gov.br
[2]Department of Chemical Engineering, of Universidade Federal do Rio Grande do Norte, UFRN,
Av. Sen. Salgado Filho 3000, CEP: 59072-970, Campus Universitário, Natal - RN, Brazil.
[3]Departament of Chemistry of Universidade Federal do Rio Grande do Norte, UFRN,
Av. Sen. Salgado Filho 3000, CEP: 59072-970, Campus Universitário, Natal - RN, Brazil.
[4]Department of Chemical Engineering of Universidade Federal de Pernambuco, DEQ,
Rua Prof. Artur de Sá, s/n, CEP: 50740-521, Cidade Universitária, Recife - PE, Brazil.

(Submitted: January 3, 2008 ; Revised: December 23, 2008 ; Accepted: January 19, 2009)

Abstract - In the present work, a synthetic effluent of phenol was treated by means of a total oxidation process—Catalyzed Wet Oxidation (CWO). A mixed oxide of Mn-Ce (7:3), the catalyst, was synthesized by co-precipitation from an aqueous solution of $MnCl_2$ and $CeCl_3$ in a basic medium. The mixed oxide, MnO_2/CeO_2, was characterized and used in the oxidation of phenol in a slurry reactor in the temperature range of 80-130ºC and pressure of 2.04-4.76 MPa. A phenol solution containing 2.4-dichlorophenol and 2.4-dichlorophenoxyacetic acid was also degraded with good results. A lumped kinetic model, with two parallel reaction steps, fits precisely with the integrated equation and the experimental data. The kinetic parameters obtained are in agreement with the Arrhenius equation. The activation energies were determined to be 38.4 for the total oxidation and 53.4 kJ/mol for the organic acids formed.
Keywords: Wet Air Oxidation; Catalyzed Wet Oxidation; Effluent; Phenol; 2,4-D; 2,4-DCP; Manganese; Cerium.

INTRODUCTION

Ever stricter enforcement of effluent quality control regulations has stimulated industries around the world to minimize their emission level of pollutants. Nevertheless, a great amount of harmful organic compounds is still produced and sent to the environment due to the inefficiency of waste management systems and/or lack of treatment altogether. The impact of industrial discharges is related to their overall features, such as biochemical oxygen demand and the amount of suspended solids, beyond their content of specific inorganic and organic toxic compounds.

Despite the large quantity of sludge, much liquid waste can be degraded using conventional biological methods of treatment. However, if the toxicity or salinity is elevated, the use of alternative methods of degradation may be needed. In some cases, even in biological systems adapted for the toxicity, high variation of organic charge can generate negative effects during treatment, causing the emission of undesirable amounts of toxic products in the resulting wastewaters. Problems of this type are solved through the use of techniques such as Wet Air Oxidation (WAO) and Catalyzed Wet Oxidation (CWO).

WAO usually works at high temperatures (400-573 K) and pressures (0.5-20 MPa). This technique

*To whom correspondence should be addressed

is the backbone of non-catalytic technology such as the Zimpro, Wetox, Vertech and Kenox process. The Nippon Shokubai Kagaku process using a monolith reactor with a Pt-Pd/TiO_2/ZrO_2 wash–coat, the Osaka Gas and the Kurita processes are some of the industrial applications of CWO (Kolaczkowski et al., 1999).

In general, the non-catalyzed and catalyzed wet oxidations present similar features in their dimensionless concentration-time profiles. In several applications, these processes have a slow conversion rate in the initial 'step' (induction period), followed by a faster stage, and finally increasing to total degradation of organic compounds contained in the liquid phase. The initial degradation step has often been cited in the scientific literature as 'the induction period', due to the time necessary to reach a critical concentration of organic radicals (Sadana and Katzer, 1974). Li, Chen and Gloyna (1991) have proposed that molecular oxygen reacts directly with phenol to produce organic radicals and hydroperoxyl radical ($HO_2^{\bullet}$). The latter is able to react with another phenol molecule to form hydrogen peroxide (H_2O_2), and, through thermal decomposition, hydroxyl radicals ($HO^{\bullet}$). Vaidya and Mahajani (2002) believe that hydroquinone may be involved in a mechanism of formation of hydroxyl and hydroperoxyl radicals that activate during the reaction, increasing the degradation rate. The hydroxyl radical has been considered the dominant oxidizing species in several degradation processes performed in acid solutions (Buxton et al., 1988).

According to Devlin and Harris (1984), phenol degradation starts with the formation of hydroquinone and catechol. These intermediates are then oxidized during the reaction to produce other organic compounds such as quinones, aldehydes and ketones. Refractory organic acids, CO_2 and tars are, in general, the end-products of the reaction.

Tars may be produced either by the polymerization of glyoxal or co-polymerization between phenol and glyoxal (Pintar and Levec, 1992). Haines (1985) reported that phenol can polymerize forming resonant structures by successive oxidative couples.

The selectivity of CO_2 formation can be affected by the catalyst type or operational conditions. In recent years, researchers have studied new efficient heterogeneous catalysts able to degrade organic effluents at low temperatures and low cost. Heterogeneous catalysts based on copper oxides such as, CuO/Al_2O_3 (Katzer, Fick and Sadana, 1976) and CuO/ZnO/CoO (Pintar and Levec, 1994) have shown remarkable efficiency in subcritical oxidation of phenol and others refractory pollutants. However, these catalysts often are leached by acid substances formed during the oxidation process, which increases the toxicity of the treated liquid waste due to the presence of copper in solution (Hocevar et al., 2000; Álvarez et al., 2001; Arena et al., 2003; Santos et al. 2004a, 2004b and 2005). Others catalysts such as Pt/TiO_2 (Maugans and Akgerman, 1997), Ru/TiO_2 (Pintar et al., 2004) and MnO_2/CeO_2 (Imamura and Doi, 1985) have been used in phenol oxidation with good results. A Mn–Ce mixed oxide (7:3) was applied by Hamoudi, Larachi and Sayari (1998) for the total degradation of phenol with the pressure of oxygen from 0.5 to 1.5 MPa and a temperature from 80 to 175ºC. The composite, compared with a 1 wt% Pt/Al_2O_3, was shown to be remarkably active for phenol removal. Apparent activation energy measuring 62 kJ/mol was obtained for the catalyst Pt/Al_2O_3 against a value of 40 for MnO_2/CeO_2. In Mn/Ce systems, it was observed that surface area alone cannot be correlated with the trend of activity change with composition and that Mn is the active species while Ce acts as a support or a promoting component (Chen et al., 2001). The same catalyst was applied to the catalytic wet oxidation of ethylene glycol by Silva, Oliveira e Quinta-Ferreira (2004). In this work the Mn–Ce mixed oxide (7:3) was compared with some commercial catalysts such as Pt/Al_2O_3, CuO–ZnO/Al_2O_3, CuO–MnOx/Al_2O_3, Fe_2O_3–MnO_x and CuO–MnO_x and other Ag–Ce–O and Ce–O catalysts prepared in laboratory. Compared with the others, the Mn–Ce–O catalyst proved to be the most active in terms of total oxidation of ethylene glycol and in relation to the total organic carbon reduction (up to 99.3%).

Among the numerous catalysts tested on model pollutants, Mn-Ce composite oxides were found to have remarkable activity in the sub-critical wet oxidation of several refractory pollutants, such as ammonia, acetic acid, pyridine and polyethylene-glycol (Imamura and Doi, 1985). Occasionally, these composites have proven to be more effective in the degradation of organic compounds than copper cations in aqueous solution (Imamura et al., 1986). Their high activity and versatility make them very promising candidates for potential industrial catalysts. For these reasons, the aim of this work is, in the first case, to show that phenol degradation can be developed in aqueous medium. For this, a parametric study of phenol aqueous degradation with MnO_2/CeO_2 catalyst in a slurry reactor was carried out and a lumped kinetic model was proposed to fit the experimental data. Secondly, to show the composite activity on a synthetic effluent containing phenol (300 mg/L), 2.4–dichlorophenol (2.4–DCP, 1000 mg/L) and 2.4–dichlorophenoxyacetic acid (2.4–D, 700 mg/L), which was tested as a

hypothetical effluent containing phenol and derivates. Similar compositions are found in raw liquid waste of industries that produce the herbicide 2,4-D. The study was developed starting from the thermal degradation of phenol carried out in a stirred reactor with temperature and pressure ranges of, respectively, 130-200ºC and 2.04-4.76 MPa. This step was important to determine in which ranges of temperature (80-110ºC) and oxygen pressure (2.04-4.76 MPa) the catalyst should be tested. Finally, the best operational conditions were applied to treat the synthetic effluent.

EXPERIMENTAL SECTION

Materials and Apparatus used in Degradation Runs

The experiments were carried out in a slurry reactor, 300-mL stainless steel high-pressure autoclave, connected to a temperature and stirring control system from Autoclave Engineers Inc. A schematic diagram of the system used in this work is shown in Fig. 1.

Phenol, 2.4–dichlorophenol (2,4–DCP) and 2.4–dichlorophenoxyacetic acid (2,4–D) were acquired from Sigma-Aldrich Chemical Co. Concentrations of phenol, 2,4-DCP and 2,4-D were monitored by means of a High Performance Liquid Chromatography (HPLC) analyzer equipped with a UV detector and a C-18 chromatographic column from Waters Co. Phenol and derivates were detected at 254 nm. The mobile phase (pH 2.95) used to separate the phenols and intermediate compounds was composed of acetonitrile (HPLC degree) and a phosphate buffer solution (4:6). Even though the HPLC analysis had been carried out, it was decided to run the experiments by following the Total Organic Carbon (TOC), because a part of the intermediates was not detected by HPLC at 254 nm. The total organic carbon contained in the liquid phase was determined using a Shimadzu TOC analyzer (5000A).

Synthesis and Characterization of the Catalyst

Manganese and cerium composite oxide with a molar ratio of 7:3 was prepared by co-precipitation from an aqueous solution of manganese (II) and cerium (III) chlorides (Sigma–Aldrich Chemical Co.). The catalyst was dried at 110ºC and calcinated under flowing air at 350ºC for 3 h according to the procedure described by Imamura and Dol (1985). Catalysts were sieved to ensure a particle with a diameter of 65 mesh.

In order to distinguish some of the properties of the MnO_2/CeO_2 composite, traditional methods for characterization were employed. The catalyst surface area was determined by the N_2 adsorption method at 77 K, in an Accusorb 77 apparatus, and the BET model. The BET specific area was measured as $120 \pm 5.0\,m^2/g$.

Thermogravimetric analyses (TG/DTA) were taken in a Perkin Elmer TGA-7 model thermal balance after the drying and calcinations of the catalyst synthesis steps. TG and DTA curves were obtained with a heating rate of 10ºC/min, in an air flow of 100 mL/min. This analysis, which happens in three steps, revealed a mass loss of the calcinated material lower than that attributed to the absorbed water, interstitial water and hydroxyl in the $Ce(H_2O)$ phase.

The specific mass of the catalyst, obtained by liquid displacement, was calculated as 3.44 kg/L.

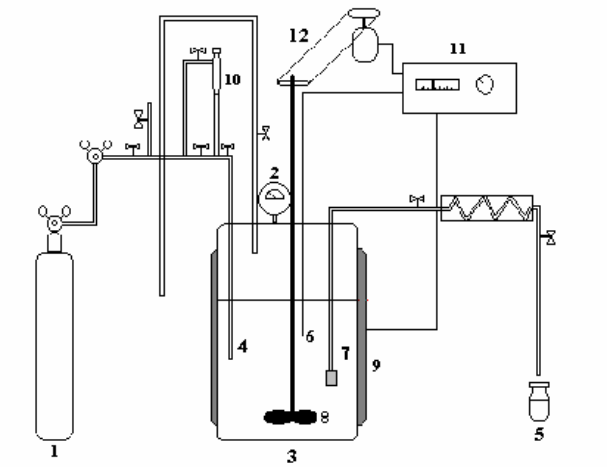

1. oxygen cylinder;
2. manometer;
3. slurry reactor;
4. oxygen distributor;
5. sample;
6. temperature sensor;
7. porous cylinder;
8. mechanic stirrer;
9. heating jacket;
10. pressure pipette;
11. temperature and rotation controller;
12. stirring device.

Figure 1: Experimental setup

Experimental Procedure of Degradation Runs

Initially the reactor was loaded with 275 mL of distilled water together with a specific amount of catalyst. The reactor was closed, the stirrer speed was set at 900 rpm and then the desired temperature was set. A purge of 10 min with pure oxygen was required to get a pure oxygen gaseous phase. The reagent injection device connected to an oxygen inlet allowed the addition of phenol—25 mL of phenol aqueous solution (25 g/L) was injected by applying an overpressure on the top of the pressure pipette when the desired temperature was reached. This action marked the starting time of the reaction. The operational conditions used in this work are shown in Table 1. The samples were analyzed to determine phenol and the total carbon contained in the liquid phase using HPLC and TOC analyzer.

Table 1: Range of Operating Conditions and Characteristics of the Catalyst Used in the Wet Oxidation of Phenol.

Initial phenol concentration (g/L)	2.08
Catalyst concentration (g/L)	1.26.0
Temperature range (ºC)	80200
Total pressure of the system (MPa)	2.044.76
Stirrer speed (rpm)	900
BET surface area (m^2/g)	120

RESULTS AND DISCUSSION

Effect of Temperature on the Thermal Degradation

To assess the extent of the thermal degradation of phenol, WAO tests were performed with an initial phenol concentration of 2.08 g/L, in the absence of the heterogeneous catalyst, at temperatures of 130, 160 and 200ºC while the pressure of oxygen was maintained at 3.40 MPa. The experimental results are shown in Fig. 2.

The dimensionless thermal degradation profiles (Fig. 2) show that temperature strongly influences pollutant removal. The WAO process was more effective for phenol abatement when carried out at 200ºC. Within 15 minutes of the reaction, the reacted phenol observed at 130ºC (5 %) and 160ºC (6 %) was very slight compared to that obtained at 200ºC (99 %). The reaction does not occur at 130ºC because this temperature is most likely unable to induce the formation of free radical species.

Effect of Pressure on Thermal Degradation

The system was tested in relation to the effect of pressure on phenol removal. An oxygen pressure range of 2.04-4.76 MPa was investigated to degrade the pollutant with initial concentration of 2.08 g/L at 200ºC. The results are shown in Fig. 3.

Experiments presented in Fig. 3 were set to the pressures of 2.04, 3.40 and 4.76 MPa. Curves show the total abatement of phenol in all experiments after 40 minutes of reaction. However, for those with less reaction time, the batch carried out at a pressure of 4.76 increased the speed of the oxidation of the pollutant. In spite of this, the profiles are just moderately affected by oxygen pressure higher than 3.4 MPa.

Both Fig. 2 and Fig. 3 show short induction periods at the beginning of the reactions, indicating a probable free radical mechanism as observed by Sadana and Katzer (1974) and Pintar and Levec (1992). In all non-catalyzed degradation experiments, colored products and tars were formed. In some runs the formation of a brownish precipitate, which may be due to the polymerization of intermediates, as described by Pintar and Levec (1992), was observed.

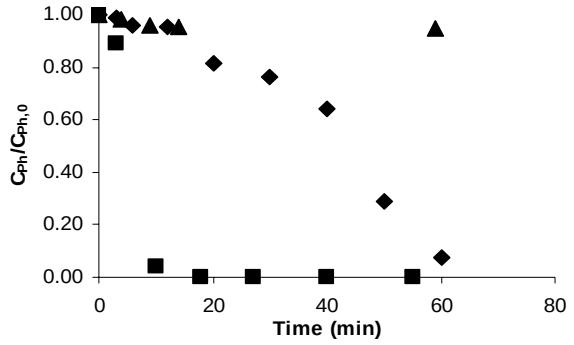

Figure 2: Residual fractions of phenol in non-catalyzed oxidation run at (▲) 130ºC, (◆)160ºC and (■) 200ºC; CPh0 = 2.08 g/L and P = 3.40 MPa.

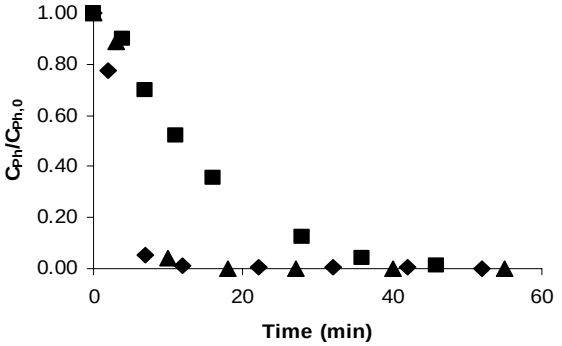

Figure 3: Residual fractions of phenol in non-catalyzed oxidation run at (■) 2.04 MPa, (▲) 3.40 MPa and (◆) 4.76 MPa; CPh0 = 2.08 g/L and T =200 ºC.

Effect of Temperature on Catalyzed Oxidation

For testing the activity of the catalyst, MnO_2/CeO_2, on abatement of a phenol solution, a range of temperatures at which the thermal degradation did not occur was chosen. As seen previously, non-catalyzed phenol oxidation does not occur at temperatures under 130ºC. Experiments were carried out with an initial phenol concentration of 2.08 g/L. A catalyst loading of 3.0 g/L was applied to experiments at oxygen pressure of 3.40 MPa and temperatures set to 80, 110 and 130ºC. Phenol residual fractions as a function of the time are shown at Fig. 4.

According to curves depicted in Fig. 4, experiments were moderately affected by the increasing temperature of reaction. The catalyst charge was intentionally maintained at 3.0 g/L to show the catalyst deactivation, observed by the stabilization of the phenol concentration after a time, t_d. The time to complete deactivation was 10, 15 and 35 minutes at 130, 110 and 80ºC, respectively. This shows that, in the studied range, the temperature does not influence the ultimate coke formation. Pintar and Levec (1992), Hamoudi et al. (1998) and Larachi (2001) reported that catalyst poisoning is due to the deposition of carbon on the catalyst surface.

Effect of Pressure on Catalyzed Oxidation

The pressure range studied in phenol catalyzed oxidation was the same as that in phenol thermal degradation, i.e., 2.04 MPa, 3.40 MPa and 4.76 MPa. The experiments were carried out at 130ºC, an initial phenol concentration of 2.08 g/L and a catalyst loading of 3.40 g/L. The results are shown in Fig. 5.

The batches show only a slight pressure influence on the phenol curves at up to 10 minutes of reaction. A possible explanation may be that even the lowest oxygen pressure (2.04 MPa) is enough to maintain a large excess of oxygen in the aqueous phase. Thus, when an oxygen molecule reacts in the liquid phase, it is quickly substituted by another transferred from the gas phase due to the severe hydrodynamic conditions. The three profiles in Fig. 5 reach practically the same residual value—consequence of the deposit formation on the catalyst surface.

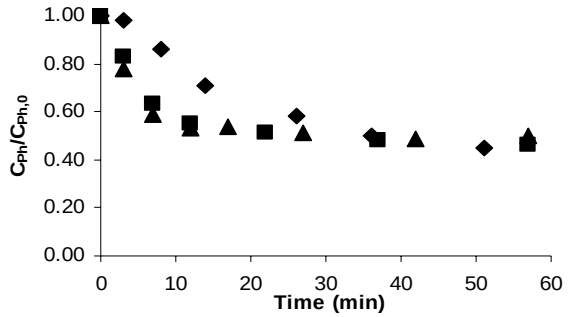

Figure 4: Dimensionless concentration-time profiles of phenol CWO at temperatures of (◆) 80ºC, (■) 110ºC and (▲) 130ºC; C_{Ph0} = 2.08 g/L, m_C = 3.0 g/L and P = 3.40 MPa.

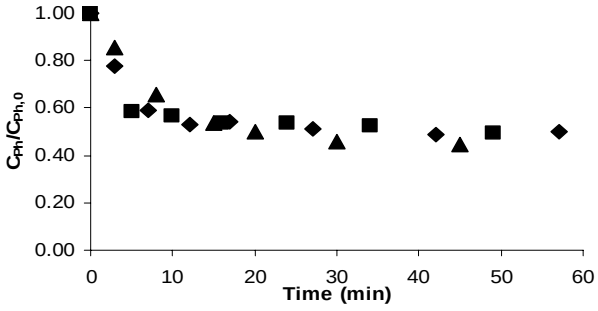

Figure 5: Dimensionless concentration-time profiles of phenol CWO at pressures of (▲) 2.04 MPa (◆) 3.40 MPa and (■) 4.76 MPa; C_{Ph0} = 2.08 g/L, m_C = 3.0 g/L and T = 130ºC.

Effect of Catalyst Loading on Catalyzed Oxidation

The influence of catalyst loading was investigated in three runs at the same initial phenol concentration (2.08 g/L). The temperature was maintained fixed at 130ºC and pressure at 3.40 MPa. The results are shown in Fig. 6.

The initial slopes of the curves in Fig. 6 reveal that the initial degradation rate is practically independent of the catalyst charge. This behavior may be attributed to the homogeneous-heterogeneous degradation mechanism of organic compounds reported in several studies (Pintar and Levec, 1992; Li, Chen and Gloyna, 1991; Vaidya and Mahajani, 2002). Indeed, if the generation of hydro-radicals occurs on the catalytic surface, with reaction in the homogeneous phase, considering the scavenging which normally happens, this could result in the independence of the initial reaction rate as observed in Fig. 6. Also, the curves show that the final concentration of phenol is strongly dependent on the catalyst loading, which is a consequence of the number of available catalytic sites, i.e., the higher the charge of the catalyst the more time it will take for the complete obstruction of the sites. Similar results were found by Hamoudi, Larachi and Sayari (1998).

Degradation of a Composed Synthetic Effluent

A synthetic effluent formed by phenol, 2,4-D and 2,4-DCP acid with initial concentrations of 0.3 g/L, 0.7 g/L and 1.0 g/L, respectively, was treated using the same technique. The experiments were carried out at 130ºC and 3.40 MPa with a catalyst loading of 6.0 g/L. The experimental results are shown in Fig. 7.

Profiles depicted in Fig. 7 show that 2.4-DCP is more easily degraded in presence of MnO_2/CeO_2 when compared with phenol and 2.4-D. A possible reason can be attributed to the formation of ternary free radicals in the oxidation process of 2.4-DCP. As the current literature thoroughly describes, these radicals are more stable than secondary radicals produced in the oxidation of phenol; consequently, they have more time to promote the reaction. The herbicide 2.4-D is also substituted in the ortho- and para- positions, however the degradation rate is lower than phenol and 2.4-DCP. The apparent inconsistency can be resolved if the 2.4-D oxidation starts in the aliphatic radical bonded to the aromatic ring through the oxygen atom.

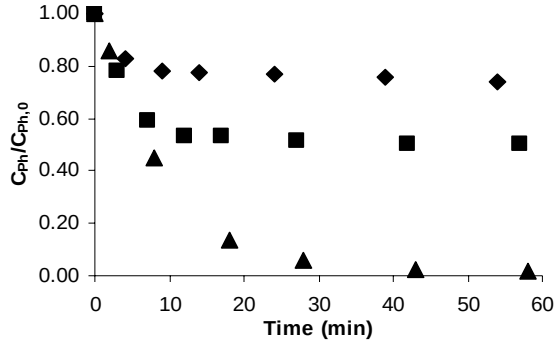

Figure 6: Residual fractions of phenol in three experiments catalyzed by MnO_2 /CeO_2 at loading of (◆) 1.2 g/L, (■)3.0 g/L, (▲) 6.0 g/L; C_{Ph0} = 2.08 g/L, T = 130ºC and P = 3.40 MPa.

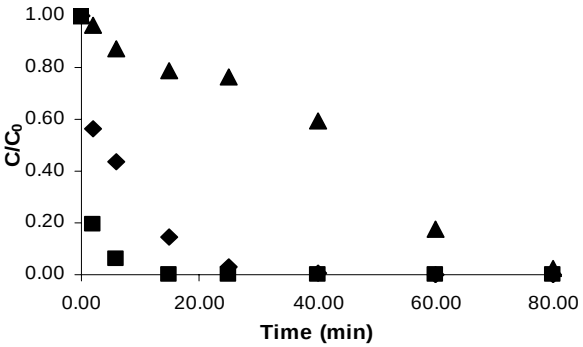

Figure 7: Dimensionless concentration-time profiles of (◆) Phenol, (▲) 2,4–D and (■) 2,4–DCP; C_{Ph} = 0.3 g/L, $C_{2,4D}$ = 0.7 g/L, $C_{2,4DCP}$ = 1.0 g/L, m_C = 6.0 g/L, T = 130ºC and P = 3.40 MPa.

A Lumped Kinetic Model

A total oxidation mechanism for the degradation of organic compounds is often very complex. To elaborate an accurate model, it would be necessary to know all intermediates and final products involved in the reaction. In the present work, this problem was solved with a lumped kinetic model. In this model some species are grouped according to their susceptibility to oxidation and normalized by a common element, carbon.

TOC analyzer was used to measure the carbon concentration owing to the phenol and intermediates contained in the liquid phase. TOC data, used as a function of time, was correlated through the lumped kinetic model first proposed by Maugans and Akgerman (1997). According to Zhang and Chuang (1999), this model can be used for both catalytic and non-catalytic wet oxidation processes.

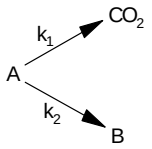

The "lumps" seen in the kinetic model are the phenol and non-refractory substances group (A) and the refractory products group (B). The dimensionless carbon concentrations were thus calculated:

$$C_A = \frac{\left[\begin{array}{c}\text{phenol and non-refractory}\\ \text{substances carbon group}\end{array}\right]}{[TOC]_0} \quad (1)$$

$$C_B = \frac{[\text{refractory products carbon group}]}{[TOC]_0} \quad (2)$$

From the proposed model, the following equations were derived:

$$-\frac{dC_A}{dt} = (k_1 + k_2)\cdot C_A \quad (3)$$

$$\frac{dC_B}{dt} = k_2 \cdot C_A \quad (4)$$

Equations 3 and 4 were solved by taking into account the dimensionless carbon concentration shown in Eq. 1 and Eq. 2. Thus, the integrated equations that describe the residual fractions, the lumps A and B, as a function of time are:

$$C_A = C_{A0}\cdot \exp\left[-(k_1 + k_2)\cdot t\right] \quad (5)$$

$$C_B - C_{B0} = \frac{C_{A0}\cdot k_2}{k_1 + k_2}\left\{1 - \exp\left[-(k_1 + k_2)\cdot t\right]\right\} \quad (6)$$

Equations 5 and 6 were combined to give:

$$C_r = \frac{TOC}{TOC_0} = C_A + C_B \quad (7)$$

C_r corresponds at the total organic carbon contained in the liquid phase. Finally, from the initial conditions t= 0, C_{A0}= 1 and C_{B0}= 0, the following equation can be obtained:

$$C_r = \frac{k_2}{k_1 + k_2} + \frac{k_1}{k_1 + k_2}\cdot \exp\left[-(k_1 + k_2)\cdot t\right] \quad (8)$$

Equation 8 was fit to experimental data using the mathematical software Mathcad 2000 Professional through the *genfit* subroutine. The results can be seen in Fig. 8. This routine returns a vector containing the parameters that make a generic function of t and n parameters (k_1...k_n) that best approximate the experimental data in vx and vy. The *genfit* routine employs the Levenberg-Marquardt method for minimization.

It is evident that the Lumped Kinetic model fits the experimental data with great precision, although it does not include the carbonaceous deposits formation. This limitation is compensated by the simplicity and easy implementation of the model. The parameters are shown in Table 2 for three temperatures which have been studied.

The curves presented in Fig. 9 (Arrhenius plots) show that the formation steps of intermediates (B) and CO_2 have similar activation energies. Moreover, the kinetic constants, k_1 and k_2, demonstrate a good agreement with the Arrhenius Law with correlation coefficients of 0.96 and 0.98 respectively. In Table 3, the activation energies obtained in this work are compared with results presented in the literature.

Concerning the CO_2 production step, the value 38.4 kJ/mol is in accordance with the activation energy obtained by Hamoudi et al. (1998) for the total phenol oxidation using the same type of reactor, the same catalyst and similar operational conditions. The value 53.4 kJ/mol represents the activation energy for the formation step of refractory intermediate and it is in accordance with the value of 48.3 kJ/mol determined by Ding et al. (1995) in the temperature range 117-137ºC and pressure of 4.0 MPa.

The agreement observed between the energies calculated and those published in the current literature reinforce the reliability of the proposed model to describe Catalyzed Wet Oxidation of phenol through a simplified mechanism.

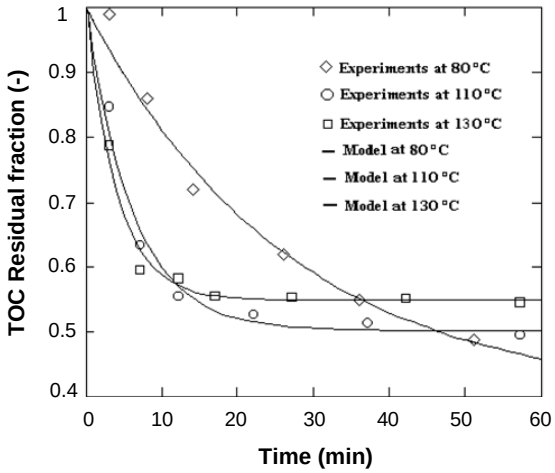

Figure 8: Lumped Kinetic Model fitting to TOC experimental data of aqueous phenol solution catalyzed by MnO_2 /CeO_2 at loading of 3.0 g/L; P = 3.40 MPa and C_0 = 3.0 g/L.

Table 2: Parameters calculated from the Lumped Kinetic Model.

Parameters	80°C	110°C	130°C
k1 (min-1)	0.023	0.082	0.111
k2 (min-1)	0.015	0.083	0.136

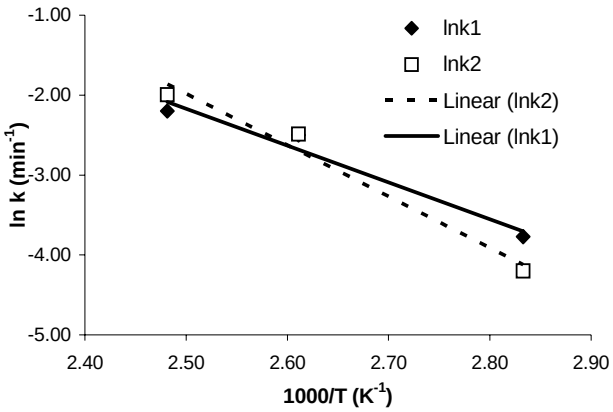

Figure 9: Arrhenius curves: ln k versus 1000/T.

Table 3: Activation energies calculated from the Arrhenius curves in comparison with data in the current scientific literature.

	Hamoudi et al. (1998)	Ding et al. (1995)	Present work
E_1 (kJ/mol)	40.0	–	38.4
E_2 (kJ/mol)	–	48.3	53.4

CONCLUSION

Efficient oxidation of phenol occurs in the presence of the catalyst MnO_2/CeO_2. The total removal of phenol was achieved within 40 minutes of reaction at 130ºC and a catalyst loading of 6.0 g/L, reaffirming that this technique is a good alternative to phenol oxidation in the liquid phase.

The manganese-cerium mixed oxide has demonstrated its efficiency for the phenol, 2.4-DCP and 2,4-D total oxidation. Thus, a CWO system could be considered for the abatement of an aqueous waste of 2.4-D production.

The Lumped Kinetic Model composed of two parallel steps — total oxidation to CO_2 and partial oxidation to refractory intermediates — fits the

experimental data accurately representing remaining TOC profiles in the range of 80-130ºC and pressure of 3.40 MPa.

ACKNOWLEDGEMENTS

The authors are grateful to the Conselho Nacional de Desenvolvimento Científico e Tecnológico (CNPq) for their financial support.

NOMENCLATURE

A	carbon group of phenol and non-refractory compounds	
B	carbon group of the refractory products	
C_A	residual fraction of Phenol and non-refractory intermediates	(-)
C_B	residual fraction of refractory products	(-)
C_{Ph}	phenol concentration	mol/L
C_r	residual fraction of TOC contained in the liquid phase	(-)
k_1, k_2	kinetic parameters	min^{-1}
E_1, E_2	activation energy	kJ/mol
t	reaction time	min
TOC	Total Organic Carbon	mg/L

REFERENCES

Álvarez, P., McLurgh, D., Kolaczkowski, S. T. and Plucinski, P., Copper oxide mounted on activated carbon as a catalyst for wet air oxidation of aqueous phenol, Sixth World Congress of Chemical Engineering Melbourne, Australia (2001).

Arena, F., Giovenco, R., Torre, T., Venuto, A. and Parmaliana, A., Activity and resistance to leaching of Cu-basedcatalysts in the wet oxidation of phenol, App. Catal. B: Environ., 45, p. 51 (2003).

Buxton, G. V., Greenstock, C. L., Helman, W. P. and Ross, A. B., Critical Review of Rate Constants for Reactions of Hydrated Electrons, Hydrogen atoms and hydroxyl radicals in aqueous solution, J. Phys. Chem. Ref. Data, 17, p. 513 (1988).

Chen, H., Sayari, A., Adnot, A. and Larachi, F., Composition–activity effects of Mn–Ce–O composites on phenol catalytic wet oxidation, App. Catal. B. Environ., 32, p. 195 (2001).

Devlin, H. R. and Harris, I. J., Mechanism of the Oxidation of Aqueous Phenol with Dissolved Oxygen, Ind. Eng. Chem. Fundam., 23, p. 387 (1984).

Ding, Z. Y., Aki, S. N. V. K. and Abraham, M. A., Catalytic supercritical water oxidation: phenol conversion and product selectivity, Environ. Sci. Technol., 29, p. 2748 (1995).

Haines, A. H., Methods for the oxidation of organic compounds (best synthetic methods), Academic Press, Inc., Orlando, Florida, p. 195 (1985).

Hamoudi, S., Larachi, F. and Sayari, A., Wet oxidation of phenolic solution over heterogeneous catalysts: degradation profile and catalyst behaviour, J. Catal., 177, p. 247 (1998).

Hocevar, S., Krasovec, U. O., Orel, B., Aricó, A. S. and Kim, H., CWO of phenol on two differently prepared $CuO–CeO_2$ catalysts, App. Catal. B: Environ., 28, p. 113 (2000).

Imamura, S. and Doi, A., Wet oxidation of ammonia catalyzed by cerium-based composite oxides, Ind. Eng. Chem. Prod. Res. Dev, 24, p. 75 (1985).

Imamura, S., Nakamura, M., Kawabata, N., Yoshida, J., Ishida, S., Wet Oxidation of Poly(ethylene Glycol) Catalyzed by Manganese-Cerium Composite Oxide, Ind. Eng. Chem. Prod. Res. Dev., 25, p. 34 (1986).

Katzer, J. R., Ficke, H. H. and Sadana, A., Evaluation of aqueous phase catalytic oxidation. J.-Water Pollut. Control Fed., 48 (5), p. 920 (1976).

Kolaczkowski, S. T., Plucinski, P., Beltran, F. J., Rivas, F. J. and McLurgh, D. B., Wet air oxidation: a review of process technologies and aspects in reactor design, Chem. Eng. J., 73, p. 143 (1999).

Larachi, F., Neural network kinetic prediction of coke burn-off on spent MnO_2/CeO_2 wet oxidation catalysts, App. Cat. B: Environ., 30, p. 141 (2001).

Li, L., Chen, P. and Gloyna, E. F., Generalized kinetic model for wet oxidation of organic compounds, AIChE Journal, 37 (11), p. 1687 (1991).

Maugans, C. B. and Akgerman, A., Catalytic wet oxidation of phenol over a Pt/TiO_2 catalyst, Water Res., 31(12), p. 3116 (1997).

Pintar, A. and Levec, J., Catalytic liquid-phase oxidation of phenol aqueous-solutions - a kinetic investigation, Ind. & Eng. Chem. Res., 33(12), p. 3070 (1994).

Pintar, A. and Levec, J., Catalytic oxidation of organics in aqueous solutions. 1. kinetics of phenol oxidation, J. Catal., 135, p. 345 (1992).

Pintar, A., Bercic, G., Besson, M. and Gallezot, P., Catalytic wet-air oxidation of industrial effluents: total mineralization of organics and lumped

kinetic modeling, App. Catal. B: Environ. 47, p. 143 (2004).

Sadana, A. and Katzer, J. R., Involvement of free-radicals in aqueous-phase catalytic-oxidation of phenol over copper oxide, J. Catal., 35(1), p. 140 (1974).

Santos, A., Yustos, P., Quintanilla, A., Garcia-Ochoa, F., Casas, J. A. and Rodríguez, J. J., Evolution of toxicity upon wet catalytic oxidation of phenol, Environ. Sci. and Technol., 38, p. 133 (2004a).

Santos, A., Yustos, P., Quintanilla, A. and Garcia-Ochoa, F., Lower toxicity route in catalytic wet oxidation of phenol at basic pH by using bicarbonate media, App. Catal. B: Environ., 53, p. 181 (2004b).

Santos, A., Yustos, P., Quintanilla, A. and Garcia-Ochoa, F., Influence of pH on the wet oxidation of phenol with copper catalyst, Topics in Catalysts, 33, p. 181 (2005).

Silva, A. M. T., Oliveira, A. C. M. and Quinta-Ferreira, R. M., Catalytic wet oxidation of ethylene glycol: kinetics of reaction on a Mn–Ce–O catalyst, Chemical Engineering Science 59, p. 5291 (2004).

Vaidya, P. D. and Mahajani, V. V., Insight into sub-critical wet oxidation of phenol, Adv. Environ. Res., 6, p. 429 (2002).

Zhang, Q. and Chuang K. T., Lumped kinetic model for catalytic wet oxidation of organic compounds in industrial wastewater, AIChE Journal, 45(1), p. 145 (1999).